doi:10.1246/cl.2010.347
Published on the web March 6, 2010

Determination of Easy Magnetization Axis of Mordenite Zeolite

Chika Matsunaga,[1,2] Tetsuo Uchikoshi,[2] Tohru S. Suzuki,[2] Yoshio Sakka,[2] and Motohide Matsuda*[1]
[1]*Graduate School of Science and Technology, Kumamoto University, 2-39-1 Kurokami, Kumamoto 860-8555*
[2]*Nano Ceramics Center, National Institute for Materials Science, 1-2-1 Sengen, Tsukuba 305-0047*

(Received December 25, 2009; CL-091148; E-mail: mm_2008@alpha.msre.kumamoto-u.ac.jp)

The easy-magnetization axis of mordenite zeolite was determined using commercially available mordenite powder. The well-dispersed suspension of the powder was consolidated by slip casting in a 12-T static magnetic field. The thick bulk deposit was cut into a dice in order to investigate the XRD patterns from the mutually orthogonal surfaces of the consolidated mordenite compacts, the normal lines of which surfaces were parallel and perpendicular to the applied magnetic field. The easy-magnetization axis of mordenite was determined to be the *b* axis based on the XRD measurements.

Many materials possessing anisotropic crystal structures generally show anisotropic physical and chemical properties and have a functionally superior crystallographic axis and/or plane. The formation of a crystalline oriented microstructure is crucial for those materials to show anisotropy. A magnetoscientific method has been one of the most useful techniques for the preparation of crystalline oriented materials. In principle, magnetic crystalline orientation occurs only in materials having magnetization anisotropy and is achieved when the magnetic orientation energy, $\Delta E = \Delta\chi VB^2/2\mu_0$, exceeds the thermal energy, k_BT, where $\Delta\chi$ is the difference in the magnetic susceptibilities between the axes of easy and difficult magnetization, V is the volume of the material, B is the applied magnetic field, μ_0 is the permeability in a vacuum, and k_B is the Boltzmann constant.[1–3]

Mordenite is a high-silica zeolite with an ideal composition of $Na_8Al_8Si_{40}O_{96}\cdot nH_2O$.[4,5] It has been used for adsorptive separation and catalytic reactions such as dewaxing, isomerization, and alkylation.[6–8] Mordenite has an orthorhombic column framework with two-dimensional pores. The pore system consists of two different pore channels; i.e., elliptical main channels composed of a 12-membered ring (0.67×0.70 nm^2) running along the *c* axis, and the other composed of an eight-membered ring (0.26×0.57 nm^2) running along the *b* axis.[4,5] This anisotropic framework structure leads to anisotropic functional properties. The orientated film of mordenite, whose surface is normal to the specific pore channels, is a desirable form because such an orientation leads to the ready access of selected reactant molecules to the pore channels for separation and catalytic reactions. Secondary growth is one fabrication method for oriented zeolite films. Fine seed crystals are applied on a substrate, and then the seeded substrate is hydrothermally treated in a reaction sol.[9–13] The microstructures of the resultant zeolite films are generally dominated by the seeding process. If the selected axis of mordenite is aligned normal to the substrate in the seeding process, it may lead to fabrication of the mordenite film with oriented pore channels.

Magnetic orientation is likely to be effective for the preparation of crystalline oriented mordenite polycrystalline films. The pore channels of mordenite run along the *b* and *c* axes; therefore, the *b* or *c* axis alignment is attractive to make full use of the pore channels. However, this technique is not applicable without knowing the easy-magnetization axis of mordenite. In general, the easy-magnetization axis of an anisotropic material is determined using a vibrating sample magnetometer (VSM) or a superconducting quantum interference device (SQUID), for a single crystal of the material. However, it is difficult to get such a large single crystal of mordenite zeolite. The purpose of this study is to determine the easy-magnetization axis of mordenite zeolite using commercially-available mordenite powder.

The mordenite powder used in this study was a highly siliceous H^+-type mordenite zeolite (HSZ-640HOA, Tosoh Co., Ltd.; $SiO_2/Al_2O_3 = 230$). Figure 1 shows the XRD pattern of the as-received mordenite powder, which has good crystallinity. The powder was dispersed in distilled water by ultrasound, and then the suspension was stored for 3 days without stirring to remove any agglomerated large particles by gravitational sedimentation. Figure 2 shows the SEM image of the mordenite powder after the sedimentation classification. The well-dispersed primary particles were found to be platelets. The ζ potential of the mordenite measured by Doppler laser was -53 mV. The collected supernatant suspension was consolidated by slip casting in a static magnetic field of 12 T. A superconducting magnet (JMTD-12T100NC5, Japan Superconductor Tech., Inc.) was the source of the strong magnetic field. The direction of the magnetic field was parallel or perpendicular to the casting direction. During the slip casting, the crystallographic axis of the highest χ, the easy-magnetization axis of the mordenite, is aligned parallel to the direction of the applied static magnetic

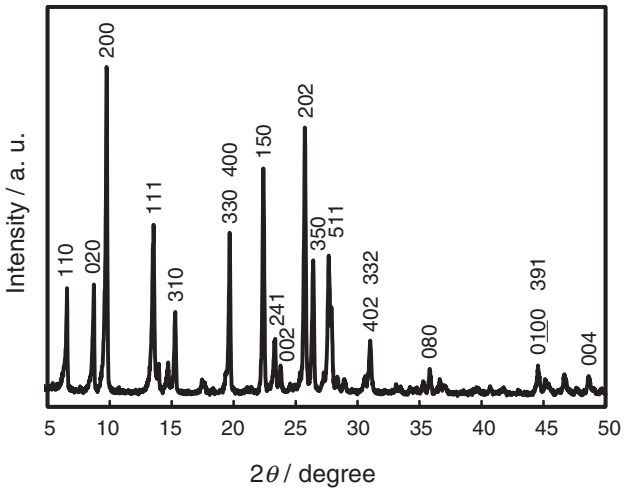

Figure 1. XRD pattern of the as-received mordenite powder.

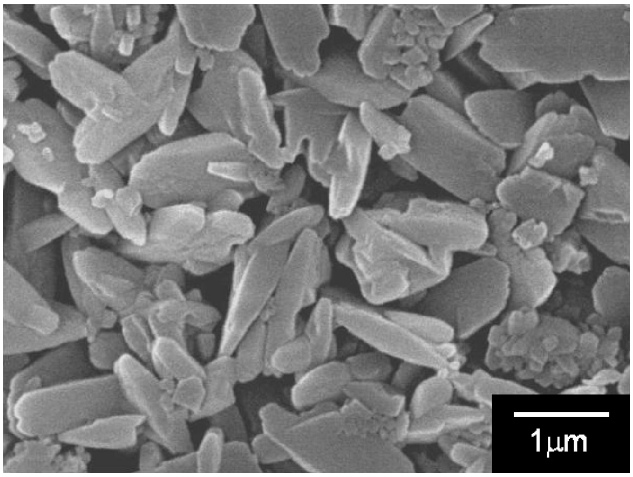

Figure 2. SEM image of mordenite powder after the sedimentation classification.

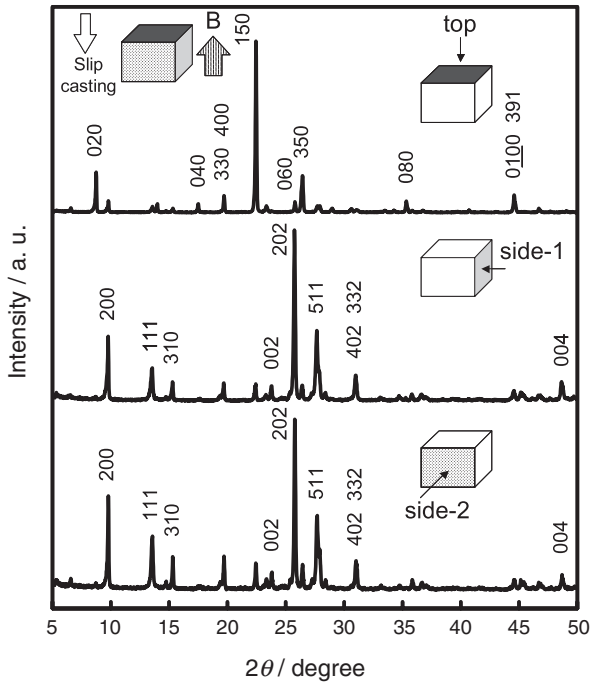

Figure 3. XRD patterns of the top and side surfaces of a bulk consolidated in a vertically applied static magnetic field which is parallel to the casting direction.

field, and the oriented particles sediment into a thick cake. The green cake was kept in the magnetic field until completion of the slip casting. The thick bulk deposit with a thickness of ca. 5 mm was removed from the magnetic field and then cut into a dice in order to investigate the XRD patterns from the mutually orthogonal surfaces of the consolidated mordenite compacts, the normal lines of which surfaces are parallel and perpendicular to the applied magnetic field.

Figure 3 shows the XRD patterns of the top and side surfaces of the bulk compact deposited in a vertically applied static magnetic field which is parallel to the casting direction. As

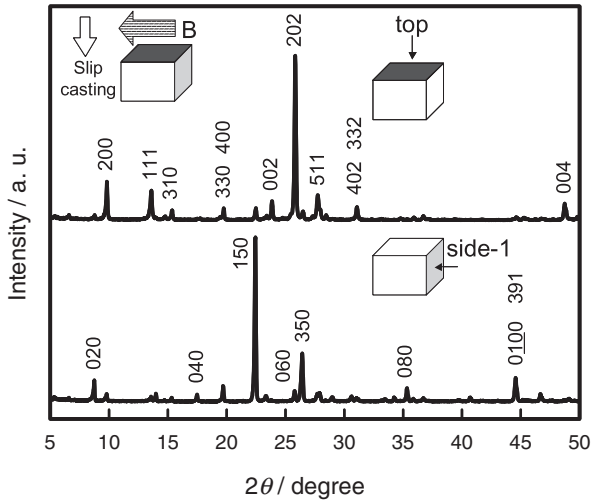

Figure 4. XRD patterns of the top and side surfaces of a bulk consolidated in a horizontally applied static magnetic field which is perpendicular to the casting direction.

can be seen in Figure 3, the top surface has quite a different XRD pattern from the side surfaces, while the XRD patterns of side-1 and side-2 are almost the same. The characteristic peaks are 020, 040, 150, 060, 350, 080, and $0\underline{1}00$ reflections from the top surface and 200, 111, 310, 002, $20\underline{2}$, 511, 402, and 004 reflections from the side surfaces. Since the XRD peaks indicated a high likelihood of the b axis orientation, the interplanar angles ϕ between the (hkl) planes and the ($0k0$) plane was calculated for the orthorhombic cell of the mordenite-type zeolite ($a = 1.811$ nm, $b = 2.053$ nm, $c = 0.7528$ nm). The interplanar angle ϕ between the planes ($h_1k_1l_1$) and ($h_2k_2l_2$) for an orthorhombic cell is given by the following equation.[14]

$$\cos\phi = \frac{\dfrac{h_1h_2}{a^2} + \dfrac{k_1k_2}{b^2} + \dfrac{l_1l_2}{c^2}}{\sqrt{\left(\dfrac{{h_1}^2}{a^2} + \dfrac{{h_1}^2}{b^2} + \dfrac{{l_1}^2}{c^2}\right)\left(\dfrac{{h_2}^2}{a^2} + \dfrac{{k_2}^2}{b^2} + \dfrac{{l_2}^2}{c^2}\right)}} \quad (1)$$

The diffraction peaks of the planes ($0k0$) ($\phi_{0k0} = 0°$) ($k = 2$, 4, 6, 8, and 10) appear only for the top, and the peaks of the (150) ($\phi_{150} = 12.8°$) and (350) ($\phi_{350} = 34.2°$) planes of the top are stronger than those of the side. In contrast, the diffraction peaks of the (200) ($\phi_{200} = 90°$), (002) ($\phi_{002} = 90°$), (202) ($\phi_{202} = 90°$), (402) ($\phi_{402} = 90°$), (004) ($\phi_{004} = 90°$), (511) ($\phi_{511} = 81.9°$), (310) ($\phi_{310} = 73.7°$), (111) ($\phi_{111} = 71.3°$), and (332) ($\phi_{332} = 65.0°$) planes of the side are stronger than those of the top. The XRD data clearly show that all the dominant reflection peaks from the top surface have lower tilting angles with the ($0k0$) plane, and those from the side surface have 90° or closer tilting angles with the ($0k0$) plane. Figure 4 shows the XRD patterns of the top and side-1 surfaces of a bulk consolidated in a horizontally applied magnetic field; the side-1 is perpendicular to the direction of the strong magnetic field. The tendency of the XRD patterns for the top and side surfaces of Figure 4 is similar to that of the side and top of Figure 3, respectively. These results show that the b axis of mordenite is an easy-magnetization axis because the b axis of the mordenite is aligned parallel to the direction of the applied strong magnetic field. For the top surface

in Figure 3 and the side surface in Figure 4, the 150 reflection is stronger than the 020. This may be because partial overlapping of the edges of the platelet-like particles is inevitable during the consolidation process.

In summary, the consolidated compacts of mordenite particles were obtained by slip casting in a 12-T static magnetic field. The easy-magnetization axis of mordenite was revealed to be the *b* axis based on XRD measurements.

The authors wish to thank Ms. N. Hatahoko at Kumamoto University for her help with SEM observations. This work was partially supported by Grant-in-Aid for Scientific Research (C) (No. 2056062600) from Japan Society for the Promotion of Science (JSPS).

References

1 P. de Rango, M. Lees, P. Lejay, A. Sulpice, R. Tournier, M. Ingold, P. Germi, M. Pernet, *Nature* **1991**, *349*, 770.
2 T. Uchikoshi, T. S. Suzuki, Y. Sakka, *J. Mater. Sci.* **2006**, *41*, 8074.
3 Y. Sakka, T. S. Suzuki, *J. Ceram. Soc. Jpn.* **2005**, *113*, 26.
4 W. M. Meier, *Z. Kristallogr.* **1961**, *115*, 439.
5 M. M. J. Treacy, J. B. Higgins, *Collection of Simulated XRD Powder Patterns for Zeoliotes (Fifth revised edition)*, Elsevier Science, **2007**.
6 H. Igarashi, H. Uchida, M. Watanabe, *Chem. Lett.* **2000**, 1262.
7 A. Shaikh, P. N. Joshi, N. E. Jacob, V. P. Shiralkar, *Zeolites* **1993**, *13*, 511.
8 H. Toshio, H. Katsumi, EP Patent 1077084A2, **2001**.
9 A. Gouzinis, M. Tsapatsis, *Chem. Mater.* **1998**, *10*, 2497.
10 J.-C. Lin, M. Z. Yates, *Chem. Mater.* **2006**, *18*, 4137.
11 G. N. Karanikolos, J. W. Wydra, J. A. Stoeger, H. García, A. Corma, M. Tsaparsis, *Chem. Mater.* **2007**, *19*, 792.
12 T. Ban, J. Morimoto, Y. Ohya, *Mater. Chem. Phys.* **2008**, *109*, 347.
13 M. Matsukata, K. Sawamura, T. Shirai, M. Takada, Y. Sekine, E. Kikuchi, *J. Membr. Sci.* **2008**, *316*, 18.
14 B. D. Cullity, *Elements of X-ray Diffraction*, 2nd ed., Addison Wesley Publishing Company, **1978**, appendix 3–3.

